DOI:10.1478/C1A0701001

Atti dell'Accademia Peloritana dei Pericolanti
Classe di Scienze Fisiche, Matematiche e Naturali
Vol. LXXXV, C1A0701001 (2007)
Adunanza del 15 maggio 2006

MELTING LINE OF KRYPTON IN EXTREME THERMODYNAMIC REGIMES

EMANUELA GIUFFRÉ [a] AND FRANZ SAIJA *[b]

(Nota presentata dal Socio Ordinario Cirino Vasi)

ABSTRACT. We have performed extensive computer simulations of the thermodynamic and structural properties of the krypton rare gas modeled by the modified Buckingham exponential-6 interatomic potential. Using a new set of potential parameters, we have found a good agreement with the room temperature equation of state at very high pressure obtained by diamond anvil cell experiments. Moreover, the melting line of the model has been estimated through the Lindemann criterion; the agreement with the low-pressure experiments is excellent, whereas at higher pressure, the model poorly reproduces the typical softening of the experimental melting curve.

1. Introduction

In the last decade a renewed interest in the properties of rare gases (RG) at high pressures and temperatures (HP/HT) has emerged, mainly because new sophisticated equipments, like the Laser-Heated Diamond Anvil Cell [1], made available new experimental results at these extreme thermodynamic conditions. These experiments have shown an unexpected behaviour in the melting line of heavier rare gases like Argon, Krypton and Xenon [2, 3, 4]. Anomalous features have also emerged in the composition of terrestrial atmosphere, in particular the little abundance of Xenon with respect to the lighter Argon and, especially, Krypton. This phenomenon is known as "missing Xenon paradox" [5, 6] and in order to be explained some hypothesis have been proposed. One of these hypothesis is based on the possibility that RG degassed from the interior of the Earth and for some reason the Xe remained trapped deep inside the planet. In favour of such scenario, the high pressure experiments mentioned above show that Ar, Kr and Xe may be solid at mantle conditions [2, 3, 4]. In these experiments the conditions found in the deep interior of the Earth are reproduced by exposing a material at pressures of hundreds of giga pascal and temperatures of thousands of Kelvin. It is known, in fact, that the pressure on the internal mantle is around 150 GPa and the temperature reaches ~ 4000 K; whereas in the core the pressure reaches ~ 300 GPa and temperature ~ 6000 K [1, 7]. In this regimes the uncertainty in the experiments is very high and also theoretical calculations face severe difficulties; as an example, recent studies have rescaled down the temperature of the internal core to 4500-5000 K [8]. In this context numerical computer simulations play an increasingly important role: on the one side, the powerful *ab-initio* numerical techniques should

be the most adequate tools to investigate the chemical-physics properties of materials under these extreme conditions [1]; on the other side, for the case at issue, preliminary classical numerical simulations may be very useful in providing new details and "economic" (from the time-consuming point of view) insights to be used for further, more complex investigations. In this work we present new and extensive classical numerical simulations of the melting line of Krypton in HP/HT regime. The outline of the paper is the following. In Sec. 2 we shortly introduce the diamond anvil cell experiments. The interatomic potential used in the computer simulations is presented in Sec. 3. In Sec. 4 we describe the Monte Carlo technique whereas Sec. 5 is devoted to presentation of results. Concluding remarks are reported in Sec. 6.

2. High pressure experiments

The melting curves of the RG solid have been measured by a variety of HP, low temperature techniques up to a few kilobars. For the heavier RG solids, where melting temperatures start to exceed the range accessible by conventional methods, diamond anvil cells turn out to be the only tool for investigating HP/HT regimes [7]. In the last decades the diamond anvil cell apparatus, invented nearly fifty years ago, has developed into a versatile tool for a broad spectrum of HP research topics, ranging from low-temperature physics to HT geoscience. Recently, the combination of HP/HT conditions, generated by two opposed diamond anvils and infrared lasers, has allowed the simulation of the planetary interiors, the discovery of new structures and behaviour in elements and the synthesis of novel hard materials [9]. With the laser-heated diamond anvil cell (LH-DAC) apparatus it is possible to reach pressures of about 200 GPa and temperatures beyond 3000 K [1]. Usually, the LH-DAC apparatus is coupled with spectroscopic instrumentations for detecting HP phase transitions using a variety of methods [1]. However, the uncertainty on this experiments is still too large and at present high-P-T research is still controversial. Results can differ significantly among major international laboratories [9].

3. The exp-6 model

It is well known that at ambient pressure and temperature the rare-gas thermal behaviour is well accounted for by the simple Lennard-Jones pair potential. However, this is not true when rare gases are very dense: the LJ potential fails in HP/HT regime. For these systems the three-body contributions to the effective potential are almost important as the pairwise contributions producing a repulsive shoulder softer than that of the LJ potential (see Fig. 1). A classical approach consists in adding explicitly the Axilrod-Teller three-body potential to an analytical function built fitting low-density experimental data [10, 11, 12]. However, it is noted that the evaluation of three-body terms is strongly time consuming. A valid alternative to these sophisticated functional forms is to use empirical effective pair potentials, parameterized using high-density experimental data [14, 15, 16, 17]. A suitable model is the exp-6 interparticle potential [18], in which the adjustable parameters include the effects of many-body interactions [19], taking into account the three-body contributions

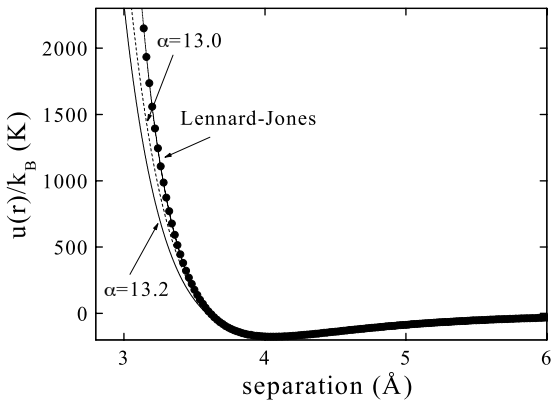

FIGURE 1. Comparison of intermolecular potential functions for Kr: The solid line is the modified Buckingham potential with $\alpha = 13.2$, ϵ/k_B = 158.3 K, $r_m = 4.056$ Å; The dashed line is the modified Buckingham potential with $\alpha = 13.0$, ϵ/k_B = 190 K, $r_m = 4.083$ Å; The solid circles represent the Lennard-Jones potential obtained using the parameters provided by Ref. [13].

TABLE 1. Interatomic potential parameters employed in the present work (k_B being the Boltzmann constant).

Potential	α	r_m or $\sigma_{\rm LJ}$ [Å]	ϵ/k_B [K]
LJ		3.680	166.7
EXP-6	13.0	4.083	190.0
EXP-6	13.2	4.056	158.3

isotropically [19, 20]. The analytical form of the exp-6 potential is:

$$v(r) = \begin{cases} +\infty & r < \sigma \\ -\frac{\epsilon}{\alpha - 6}\left\{\alpha\left(\frac{r_m}{r}\right)^6 - 6\exp\left[\alpha\left(1 - \frac{r}{r_m}\right)\right]\right\} & r \geq \sigma \end{cases} \tag{1}$$

where α controls the softness of the repulsion at small intermolecular separations and $\epsilon > 0$ is the depth of the potential minimum located at r_m. We have selected the value of σ in such a way that, for any α and r_m the function appearing in the second line of Eq. 1 reaches its maximum at σ. Hence, as r moves down to σ, $v(r)$ reaches a stationary value and then goes abruptly to infinity [21]. In Table 1 we report the parameters we have used in our numerical simulations. In Fig. 1 we compare the exp-6 potential for two different values of α (13 and 13.2) with the Lennard-Jones potential [13]. As visible, the repulsion in the

LJ interaction is stiffer than that of the exp-6 potential. This difference turns out to be not relevant at ambient pressure, but becomes crucial at high pressure. During the numerical simulations we used dimensionless variables for temperature, pressure and density, i.e., $T^* = k_{\rm B}T/\epsilon$, $P^* = Pr_{\rm m}^3/\epsilon$ and $\rho^* = \rho r_{\rm m}^3$, respectively.

4. Monte Carlo simulations

We have performed extensive Monte Carlo (MC) simulations of the exp-6 model in the canonical ensemble (*i.e.*, at constant temperature T, volume V, and number N of particles), using the standard Metropolis algorithm for sampling the equilibrium distribution in configurational space. The values of N that we have considered fit to a cubic simulation box with an integer number of cells $N = 4n^3$ for the face-centered-cubic (FCC) solid, n being the number of cells along any spatial direction. For a given particle number, the length L of the box side is adjusted to a chosen density value ρ, *i.e.*, $L = (N/\rho)^{1/3}$. If a is the distance between two nearest-neighbour reference lattice sites, we have $a = (\sqrt{2}/2)(L/n)$ for an FCC crystal. After carrying out a rigorous size dependence analysis we have studied a sample composed by $N = 864$ particle, using standard periodic boundary conditions. As a rule the last MC configuration at a given ρ has served, after suitable rescaling of particle coordinates, as the starting configuration for the run at a slightly lower density. The FCC solid path is followed until the fluid spontaneously forms during the MC run, as evidenced by the abrupt change in energy and pressure. For each ρ and T, equilibration of the sample typically takes 5×10^3 MC sweeps, a sweep consisting of one attempt to sequentially change the position of all particles. The maximum random displacement of a particle in a trial MC move has been adjusted once a sweep during the run so to keep the acceptance ratio of the moves as close as possible to 50%, with only small excursions around this value.

For given NVT conditions, the relevant thermodynamic averages have been computed over a trajectory whose length ranges from 2×10^4 to 6×10^4 sweeps. In particular, the excess energy per particle $u_{\rm ex}$, the pressure P, and the mean square deviation δR^2 of a particle from its reference lattice position have been especially monitored. Pressure comes from the virial formula,

$$P = \rho k_B T + \frac{\langle Vir \rangle}{V}\,, \quad Vir = -\frac{1}{3}\sum_{i<j} r_{ij} v'(r_{ij}) \tag{2}$$

(r_{ij} is the distance between particles i and j). In practice, in order to avoid double counting of interactions, the pair potential has been truncated above a certain cutoff distance r_c, which is only slightly smaller than $L/2$. Then, the appropriate long-range corrections have been applied to energy and pressure by assuming $g(r) = 1$ beyond r_c, $g(r)$ being the radial distribution function (RDF). The RDF histogram has been constructed with a spatial resolution of $\Delta r = r_m/50$ and updated every 10 MC sweeps.

In order to evaluate the numerical errors affecting the main statistical averages, we have divided the MC trajectory into ten blocks and estimated the length of the error bars as being twice the empirical standard deviation of the block averages from the mean (under the implicit assumption that the decorrelation time of any relevant variable is less that the

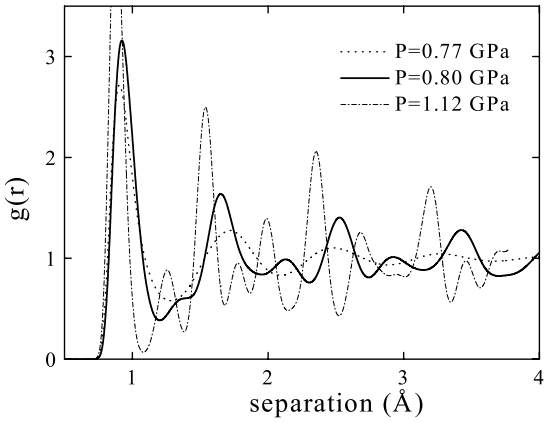

FIGURE 2. Pressure evolution of the pair distribution functions $g(r)$ of exp-6 model with $\alpha = 13.2$, ϵ/k_B = 158.3 K, $r_m = 4.056$ Å, as obtained by MC simulations at room temperature. The melting point of Kr is estimated at $P = 0.83$ GPa [22].

size of a block). Tipically, the relative errors of energy and pressure is smaller than few tenths of a percent.

5. Results and discussion

In Fig. 2 we report the pressure evolution of RDF calculated at $T = 300$ K for three different pressures ($P = 0.77, 0.80, 1.12$ GPa), using the exp-6 potential with $\alpha = 13.2$ (ϵ/k_B = 158.3 K, $r_m = 4.056$ Å). Approximately at $P = 0.80$ GPa the corresponding RDF does not show more the typical solid-like behavior (sharp and narrow Bragg's peaks) indicating that the system begins to melt (solid line in Fig. 2). This value is in excellent agreement with the experimental estimate of the Kr melting point at $T = 300$ K ($P = 0.83$ GPa [22]) and testify the reliability of the exp-6 potential at ambient temperature.

5.1. Room temperature equation of state. From the theoretical point of view the studies on the equation of state (EoS) can be classified in two categories: the zero-Kelvin quantum mechanical calculations [12, 23, 24] and the alternative approaches based on empirical or semiempirical intermolecular potentials at nonzero temperatures [10, 12, 16, 17, 25]. In this paragraph we show MC estimates of the room temperature EoS of Kr modeled through the exp-6 or LJ interatomic potentials. In Fig. 3 we report the experimental data with our MC results. The room temperature EoS (pressure-volume relationship) has been measured for solid Kr through DAC experiments up to 130 GPa [2]. In particular, we compare the pressure-volume predictions between the exp-6 with $\alpha = 13$, ϵ/k_B = 190 K, $r_m = 4.083$ Å and the LJ potential [13]. It is evident from Fig. 3 that the exp-6 potential reproduces

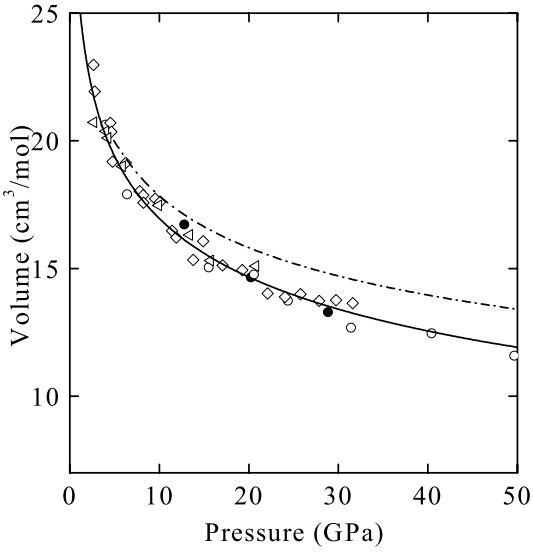

FIGURE 3. Equation of state of exp-6 potential with $\alpha = 13.0$, ϵ/k_B = 190 K, $r_m = 4.083$ Å (solid line) and of LJ potential (dash-dotted line) at $T = 300$ K. We plot also the volume data obtained through many different HP experimental techniques. Solid circles: from Fig. 1 of Ref. [2]; open circles: from Fig. 8 of Ref. [30]; diamonds: from Table I of Ref. [31]; triangles: from Ref. [32]. Uncertainties in our MC results are smaller than the symbol size.

the low- and intermediate pressure data better than the LJ potential. The agreement with different experimental results is excellent up to $P = 50$ GPa. Instead, (see Fig. 4) a new set of exp-6 parameters ($\alpha = 13.2$, ϵ/k_B = 158.3 K, $r_m = 4.056$ Å) is needed to reproduce the high-pressure data up to $P = 140$ GPa. As already observed by Ross *et al.* [19], it turns out that even a three-parameter potential is not sufficiently flexible to fit both the very high and very low pressure data.

5.2. Lindemann estimates and the melting line. In order to estimate the melting line of Krypton we have used the Lindemann criterion [26]. Of course, the one-phase indicators must be limited in their ability to yield quantitative predictions [27]. Notwithstanding their use may be very helpful in gaining qualitative information with only one-phase ingredients about the location of the phase transitions points [28].

The Lindemann ratio L is defined as the root mean square displacement of particles in a crystalline solid about their equilibrium lattice positions, divided by their nearest-neighbor

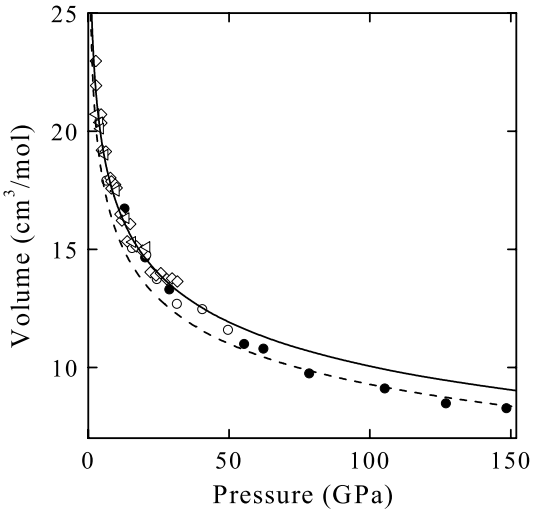

FIGURE 4. Equation of state of exp-6 potential with $\alpha = 13.0$, ϵ/k_B = 190 K, $r_m = 4.083$ Å (solid line) and with $\alpha = 13.2$, ϵ/k_B = 158.3 K, $r_m = 4.056$ Å (dashed line) at $T = 300$ K. Symbols like in Fig. 3. Uncertainties in our MC results are smaller than the symbol size.

distance a:

$$L = \frac{1}{a}\left\langle \frac{1}{N}\sum_{i=1}^{N}(\Delta\mathbf{R}_i)^2 \right\rangle^{1/2}, \tag{3}$$

where N is the number of particles and the brackets $\langle\cdots\rangle$ denote the average over the dynamic trajectories of the particles. The Lindemann criterion states that the crystal melts when L overcomes some "critical" (yet not specified *a priori*) value L_c [26]. Obviously, one hopes this latter quantity is approximately the same for different pair potentials and thermodynamic conditions. In fact, the Lindemann ratio is not universal at all, its values spanning in the range $0.12 - 0.19$. More specifically, L_c is reported to be $0.15 - 0.16$ in a FCC solid and $0.18 - 0.19$ in a body-centered-cubic (BCC) solid (see, *e.g.*, [29]).

In a recent article Saija *et al.* [27] have shown that a good choice of the Lindemann ratio value in order to detect the melting of a exp-6 FCC solid is $L_c \approx 0.15$. Since the FCC structure is known to be the stable phase for the heavier RG, we have applied the Lindemann rule to estimate the melting coexistence line in the case of Kr. Our scope is to study the pressure/temperature range of reliability of the exp-6 interatomic potential in reproducing the experimental melting boundaries. In Fig. 5 we compare our exp-6 MC results, obtained with $\alpha = 13$ (ϵ/k_B = 190 K, $r_m = 4.083$ Å) and $\alpha = 13.2$ (ϵ/k_B

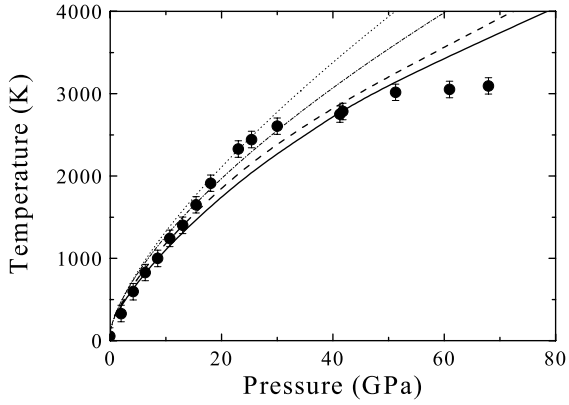

FIGURE 5. The melting points (solid circles) for Kr obtained with DAC experiments Ref. [3]. The solid and dashed lines are the Lindemann estimates obtained by MC simulations of exp-6 model with $\alpha = 13.2$ (ϵ/k_B = 158.3 K, $r_m = 4.056$ Å) and $\alpha = 13.0$ (ϵ/k_B = 190 K, $r_m = 4.083$ Å), respectively. The empirical Simon-Glatzel (dash-dotted) and modified Simon-Glatzel (dotted) equations are also plotted [7].

= 158.3 K, $r_m = 4.056$ Å), with some recent experimental melting data measured in a LH-DAC apparatus [3]. In the same plot we also report the empirical Simon-Glatzel (SG) and the modified Simon-Glatzel (mSG) equation, which are simple parametrization of melting curves. The SG relation has been shown to be related to the Lindemann law under special conditions which are expected to break down at high compressions [33]. The MC results are in good agreement with LH-DAC measurements and the predictions of the SG equations up to $P = 50$ GPa. Above these pressures, there occurs a considerable decrease in the melting slope, which seems to be a common feature for all heavier RG [3]. Very recently, Ross *et al.* [34] have shown that the bend in the melting curve in heavier RG may be due to symmetry breaking of the interatomic potential created by the $p - d$ hybridization of the outer electronic shell. More specifically, with increasing pressure the electronic configuration of heavier RG is such that neither the atom nor the interatomic potential can be easily treated as spherically symmetric objects. Probably, this quantum effect becomes prevalent in HP/HT regions making a simple two-body classical treatment unreliable.

6. Concluding remarks

In this work we have performed extensive Monte Carlo simulations of the exp-6 model, a pairwise additive spherically symmetric interparticle potential that is expected to give a realistic description of some structural properties of rare gases solid under extreme thermodynamic conditions. More specifically, we have proposed two new independent sets of

parameters for the solid Krypton rare gas which allow to reproduce accurately enough new recent diamond anvil cell experiments for the room temperature equation of state [2]. Starting from this finding we have tried to estimate through the one-phase Lindemann criterion the melting coexistence line of Krypton. As already obtained for the Xenon [21], we have found that the agreement between the exp-6 MC results and the diamond anvil cell experiments worsens with increasing temperature and pressure. Indeed, the experiments showed an anomalous lowering in the melting slope, due to quantum effects [34], that cannot be accounted for by a simple classical treatment.

References

[1] S. Scandolo and R. Jeanloz, *Am. Sc.* **91**, 516 (2003).
[2] A. P. Jephcoat, *Nature* **393**, 355 (1998).
[3] R. Boehler, M. Ross, P. Söderlind and D. B. Boercker, *Phys. Rev. Lett.* **86**, 5731 (2001).
[4] R. J. Hemley and N. W. Ashcroft, *Phys. Today* **51**, 26 (1998).
[5] R. O. Pepin, *Icarus* **92**, 2 (1991).
[6] D. Krummenacker, C. M. Merrihue, R. O. Pepin and J. H. Reynolds, *Geochim. Cosmochim. Acta* **26**, 231 (1962).
[7] M. H. Manghnani and T. Yagi (eds), *Properties of Earth and Planetary Materials at High Pressure and Temperature* (Geophysical Monograph Series, Washington, 1998).
[8] D. Alfé, G. D. Price and M. J. Gillan, *J. of Phys. and Chem. of Solids* **65**, 1573 (2004).
[9] R. Boehler, *Materials Today* **8** , 34 (2005).
[10] M. V. Bobetic, J. A. Barker, and M. L. Klein, *Phys. Rev. B* **5**, 3185 (1972).
[11] J. A. Barker, *Phys. Rev. Lett.* **52**, 230 (1986).
[12] J. H. Kim, T. Ree and F. H. Ree *J. Chem. Phys.* **91** 3133 (1989).
[13] Y. Choi, T. Ree and F. H. Ree, *Phys. Rev. B* **48**, 2988 (1993).
[14] N. H. March, "Equations of state, defects and melting" in *Molecular systems under high pressure*, edited by R. Pucci and G. Piccitto (North Holland, Amsterdam, 1991)
[15] F. H. Ree, "A new perturbation theory of solids and fluids and its applications to high-pressure melting problems" in *Molecular systems under high pressure*, edited by R. Pucci and G. Piccitto (North Holland, Amsterdam, 1991)
[16] M. Ross and A. K. McMahan, *Phys. Rev. B* **21**, 1658 (1980).
[17] M. Ross, *J. Chem. Phys.* **73**, 4445 (1980).
[18] R. A. Buckingham, *Proc R. Soc. London* **168**, 264 (1938).
[19] M. Ross, H. K. Mao, P. M. Bell and J. A. Xu, *J. Chem. Phys.* **85**, 1028 (1986).
[20] P. Loubeyre, *Phys. Rev. B* **37**, 5432 (1988).
[21] F. Saija and S. Prestipino, *Phys. Rev. B* **72**, 024113 (2005).
[22] H. Shimizu, N. Saitoh and S. Sasaki, *Phys. Rev. B* **57**, 230 (1998).
[23] J. S. Tse, V. P. Shpakov and V. R. Belosludov, *Phys. Rev. B* **58**, 2365 (1998).
[24] I. Kwon, L. A. Collins, J. D. Kress and N. Troullier, *Phys. Rev. B* **52**, 15165 (1995).
[25] U. Buck, M. G. Dondi, U. Valbusa, M. L. Klein and G. Scoles, *Phys. Rev. A* **8**, 2409 (1973).
[26] F. A. Lindemann, *Phys. Z.* **11**, 609 (1910).
[27] F. Saija, S. Prestipino and P. V. Giaquinta, *J. Chem Phys.* **124**, 244504 (2006).
[28] R. Agrawal and D. A. Kofke, *Phys. Rev. Lett.* **74**, 122 (1995); *Mol. Phys.* **85**, 23 (1995).
[29] E. J. Meijer and D. Frenkel, *J. Chem. Phys.* **94**, 2269 (1991).
[30] D. Errandonea, B. Schwager, R. Boehler and M. Ross, *Phys. Rev. B* **65** , 214110 (2002).
[31] A. Polian, J. M. Besson, M. Grimsditch and W. A. Grosshans, *Phys. Rev. B* **39**, 1332 (1989).
[32] A. Polian, J. P. Itie, E. Dartyge, A. Fontaine and G. Tourillon, *Phys. Rev. B* **39**, 3369 (1989).
[33] M. Ross, *Phys. Rev. B* **184**, 233 (1969).
[34] M. Ross, R. Boehler and P. Söderlind, *Phys. Rev. Lett.* **95**, 257801 (2005).

[a] Emanuela Giuffré
Dipartimento di Fisica
Università degli Studi di Messina
Contrada Papardo
98166 Messina, Italy

[b] Franz Saija
CNR - Istituto per i Processi Chimico-Fisici, Sezione di Messina,
Via G. La Farina, 237
98123 Messina, Italy
* **E-mail**: saija@me.cnr.it

Presented: May 15, 2006
Published on line on January 17, 2007